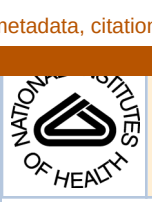

Published in final edited form as:

Angew Chem Int Ed Engl. 2011 April 11; 50(16): 3696–3700. doi:10.1002/anie.201008277.

Phosphoresent Nanoscale Coordination Polymers as Contrast Agents for Optical Imaging**

Demin Liu, **Rachel C. Huxford**, and **Wenbin Lin***

Department of Chemistry, CB#3290, University of North Carolina, Chapel Hill, NC 27599, USA

Abstract

Optical imaging, which uses neither ionizing radiation (as in X-ray computed tomography) nor radioactive materials (as in positron emission tomography or single photon emission computed tomography),[1] has emerged as a powerful imaging modality during the last two decades.[2] Optical imaging has been widely employed for oncological and other applications due to its ability to noninvasively differentiate between diseased (*e.g.*, tumor) and healthy tissues based on differential dye accumulations.[3] The need for relatively high (up to ~μM) concentrations of dyes in optical imaging, however, limits its application in many areas, such as detecting low concentrations of biological targets. For example, many biomarkers are overexpressed in the nM concentrations in diseased tissues,[4] and cannot be readily visualized by optical imaging. Dye-loaded nanoparticles represent a logical solution to lowering the detection limit due to their ability to carry a large payload of dye molecules as well as to target certain cell types by conjugation to affinity molecules. Luminescent quantum dots have indeed been extensively explored as bright and stable contrast agents for optical imaging.[5] The non-degradable nature of and the use of toxic elements in many quantum dot formulations however limit their applications in many areas. Most of fluorescent dye molecules, on the other hand, have small Stokes shifts and tend to have a significant overlap between absorption and fluorescent emission spectra. As a result, these fluorescence dyes will suffer from severe self-quenching if they are brought into close proximity with each other, as in nanoparticles with high dye loadings.

Luminescence originating from non-singlet states of metal complexes tends to have longer lifetimes and large Stokes shifts. We hypothesize that highly luminescent nanoparticles can be constructed from such dye molecules as they will not undergo self-quenching owing to the large Stokes shifts.[6,7] Herein we report the synthesis, characterization, and preliminary applications of biodegradable, phosphorescent nanoscale coordination polymers in *in vitro* optical imaging.

Coordination polymers, also called metal-organic frameworks, are an interesting class of hybrid materials constructed from metal ion or metal cluster connecting points and molecular bridging ligands.[8] Molecular tunability of such hybrid materials has allowed the design of coordination polymers for a wide range of applications, such as gas storage,[9] nonlinear optics,[10] chemical sensing,[11] and catalysis.[12] We and others recently demonstrated the ability to scale down these materials to the nano-regime to afford nanoscale coordination polymers (NCPs) for potential biological and biomedical applications.[13] For example NCPs have been shown to be applicable to biosensing,[14] magnetic resonance imaging,[15] computed tomography,[16] and drug delivery.[17] In this work, we synthesized phosphorescent NCPs using the Ru[5,5'-$(CO_2)_2$-bpy](bpy)$_2$ bridging

**We thank NIH-NCI (U01-CA151455) for financial support and Mr. Caleb A. Kent and Cheng Wang for experimental help.

*Fax: (+1)919-962-2388, wlin@unc.edu, http://www.chem.unc.edu/people/faculty/linw/wlindex.html.

ligand (bpy is 2,2'-bipyridine) and Zn^{2+} and Zr^{4+} metal-connecting points. The Zn and Zr NCPs have a dye loading of 78.7% and 57.4%, respectively. The Zr NCP was further stabilized with a silica coating and functionalized with polyethylene glycol (PEG) and a targeting molecule for *in vitro* optical imaging of cancer cells.

The phosphorescent Ru complex $\{Ru[5,5'\text{-}(CO_2H)_2\text{-bpy}](bpy)_2\}(PF_6)_2$, $[\mathbf{L}\text{-}H_2](PF_6)_2$, was synthesized by reacting 5,5'-$(CO_2Et)_2$-bpy with $Ru(bpy)_2Cl_2$, followed by acid-catalyzed hydrolysis and anion exchange. The bulk Zn coordination polymer with a formula of $[Zn_2\mathbf{L}(C_2O_4)_2]\cdot 2dmf\cdot 3H_2O$, **1**, was synthesized by reacting $Zn(NO_3)_2$ and $[\mathbf{L}\text{-}H_2](PF_6)_2$ in a dimethylformamide (dmf) and H_2O mixture in a screw-capped vial at 90 °C for 2 days. **1** crystallizes in the triclinic space group P-1, with one **L** ligand, two Zn atoms, and two oxalate molecules in the asymmetric unit.[18] The Zn center is coordinated by five oxygen atoms, one of which is from the carboxylate group of the **L** ligand, and the other four are from the oxalate molecules to form a 2D bilayer structure (Figure 1a–b). Packed along the b axis, the 2D layers have a distance of 4.8 Å between bpy planes of adjacent layers. The shortest distance between the two Ru centers within the bilayer is 9.4 Å. The phase purity of **1** is supported by a good match of the powder X-ray diffraction (PXRD) pattern of the pristine sample and the simulated pattern from the single crystal structure. The complete formulation of **1** was established by single-crystal X-ray diffraction studies, NMR analysis, and thermogravimetric analysis (TGA) results (supporting information).

Dark orange, crystalline nanoparticles of **1** (NCP-**1**) were synthesized in 54.3% yield by microwave heating of a solution of $[\mathbf{L}\text{-}H_2](PF_6)_2$, oxalic acid, and $Zn(NO_3)_2$ in dmf/H_2O at 100 °C for 5 minutes. SEM images show that NCP-**1** forms block-like particles that are approximately 100×100×50 nm in dimensions (Figure 1c). PXRD studies indicate that the NCP-**1** particles are crystalline and share the same phase as bulk crystals of **1**. UV-Vis spectrum of a dispersion of NCP-**1** in ethanol shows a broad MLCT absorption band between 400–550 nm. NCP-**1** has a luminescence quantum yield of 2.1%, with the normalized emission spectrum (λ_{max}~635 nm) shown in Figure 1d. The time-resolved emission transient for NCP-**1** monitored at 630 nm was fit to biexponential decay kinetics,[18] giving an average lifetime of 215 ns.

As the NCP-**1** particles rapidly dissolve in water and biologically relevant media, we attempted to stabilize them by encapsulation with a silica coating. The strategy of coating NCPs with a thin layer of silica was previously used by us to tune the kinetics of cargo release from NCPs.[14, 17] Silica coatings can also enhance biocompatibility and water dispersibility.[17, 20] Unfortunately, NCP-**1** was not stable under the coating conditions as the **L** dye molecules had leached from the particles and the recovered particles became nearly colorless. The decomposition of NCP-**1** under the coating conditions was corroborated by SEM and energy-dispersive X-ray spectroscopy (EDS) data (Supporting information).

We speculate that more stable NCPs can be synthesized if Zr^{4+} ions are used in place of Zn^{2+} to connect carboxylate groups of the **L** ligands, as the UiO materials composed of Zr^{4+} ions and dicarboxylate bridging ligands were shown to be among the most stable coordination polymers synthesized.[21] Microwave heating of an acidic solution of $[\mathbf{L}\text{-}H_2](PF_6)_2$ and $ZrCl_4$ in dmf at 100 °C for 10 min led to dark orange particles of NCP-**2** after centrifugation and washing with methanol and ethanol (Scheme 1). As shown in Figure 2a, SEM and TEM images showed that particles of **2** adopt a spherical morphology with an average diameter of 85 nm. NCP-**2** is amorphous as judged by the lack of peaks in the PXRD pattern. Dynamic light scattering (DLS) measurements afforded a hydrodynamic diameter of 104 ± 4 nm for particles of **2** in ethanol (Figure 2d and Table 1). The absorption and emission spectra are shown in Figure 2e; in order to eliminate scattering effects, the

absorption spectrum was also taken after digesting the NCP-**2** with sodium hydroxide (6M, aq.). **2** has a luminescent quantum yield of 0.8% and an average luminescence lifetime of 107 ns (at 630 nm). A dye loading of 57.4% and 55.0% was calculated from TGA and inductively-coupled plasma mass spectrometric (ICP-MS) results, respectively (Table 1).

The as-synthesized particles of **2** are very stable in water, but rapidly decompose in 8 mM phosphate buffered saline (PBS) at 37 °C with a half-life ($t_{1/2}$) of ~0.5 h, presumably due to the strong driving force provided by the formation of Zr phosphates. To slow down the release of **L** dye molecules from **2** in biologically relevant media, we attempted to coat the particles with a thin shell of silica. To our delight, NCP-**2** is stable under the coating conditions, and the presence of a thin layer of silica on particles of **2** after the coating procedure was confirmed by TGA, EDS (supporting information), DLS, and release profile data (Figure 2d, f, and Table 1). TGA gave a 12.5% reduction in the total weight loss for the particles of SiO_2@**2**. The DLS Z-average diameter for SiO_2@**2** is ~3 nm larger than that of **2**. SiO_2@**2** has a zeta potential of −34.4 ± 4.1 mV, which is about 22 mV more negative than that of **2** (−11.9 ± 3.2 mV). The release profile of SiO_2@**2** in 8 mM PBS at 37 °C gave a $t_{1/2}$ of 3.2 hours (Figure 2f). The half-life of SiO_2@**2** particles is long enough for preliminary optical imaging experiments with cancer cells.

Silica coatings also provide surface silanol groups for further functionalization with other molecules containing siloxy groups. Surface modification with polyethylene glycol (PEG), a relatively inert hydrophilic polymer, can prevent particle aggregation and increase the dispersibility of nanoparticles. The end of PEG chain can be further modified to contain affinity molecules that target certain biomarkers. For example, sigma-1 and sigma-2 receptors are overexpressed in a wide variety of human tumor cells,[22] which makes it possible to use sigma-receptor binding ligands, such as anisamide, for tumor targeting.[23] Therefore, SiO_2@**2** was subsequently coated with CH_3O-PEG_{2000}-$Si(OEt)_3$ or with CH_3O-PEG_{2000}-$Si(OEt)_3$ and anisamide-PEG_{2000}-$Si(OEt)_3$ in a 9 to 1 molar ratio to afford pegylated and targeted particles, PEG-SiO_2@**2** and AA-PEG-SiO_2@**2**, respectively. The PEG-SiO_2@**2** and AA-PEG-SiO_2@**2** particles appeared less aggregated (Figure 2c) and a rougher edge around the particles was observable by TEM (inset in Figure 2c). TGA gave a 1.5% increase in the total weight loss and DLS measurements gave a diameter of 122 ± 10 nm and 124 ± 7 nm and a zeta potential of −9.23±1.9 mV and −8.17± 2.8 mV, confirming the presence of the polymer coating.

To evaluate the potential use of NCP-**2** as a contrast agent for optical imaging, we conducted *in vitro* viability assays on H460 non-small cell lung cancer cells. Treatment of H460 cells with PEG-SiO_2@**2** and AA-PEG-SiO_2@**2** did not lead to any appreciable cell death after 24 h of incubation (Figure 3d). To test their *in vitro* imaging contrast efficiency and targeting capacity, laser scanning confocal fluorescence microscopy studies were performed. As shown in Figure 3a–c, significant MLCT luminescent signal was observed in the confocal z-section for H460 cells incubated with AA-PEG-SiO_2@**2**. In comparison, less luminescence was observed for H460 cells incubated with the non-targeted PEG-SiO_2@**2**. This result is further supported by an uptake study. After 24 h of incubation with H460 cells, the cells were isolated by centrifuging and washed with PBS. Cell pellets were digested in concentrated HNO_3 and Ru content was analyzed by ICP-MS. Enhanced uptake was observed for AA-PEG-SiO_2@**2** (Figure 3e).

In conclusion, we have successfully synthesized phosphorescent nanoscale coordination polymers with extremely high dye loadings. The Zr-based NCPs were stabilized with thin shells of amorphous silica to prevent rapid release from the nanoparticles, and the biocompatibility and targeting efficiency of the NCP/silica core-shell nanostructures was further improved by coating with PEG and PEG-anisamide. The anisamide-targeted particles

are efficient optical imaging contrast agents and exhibit cancer specificity as demonstrated by uptake studies and confocal microscopy of H460 cells *in vitro*. This work highlights the potential of nanoscale coordination polymers as a novel platform for designing luminescent hybrid nanoparticles with extremely high dye loadings for optical imaging.

Experimental Section

Synthesis of NCP-1

([**L**-H_2]$(PF_6)_2$ (5 mg, 0.005 mmol) and $Zn(NO_3)_2 \cdot 6H_2O$ (10 mg, 0.035 mmol) were dissolved in a mixture of dmf/H_2O (2.5mL/0.1 mL). After the addition of 15μL HCl (3M, aq.) and 5μL oxalic acid (0.75 M, dmf), the resulting solution was sealed in a microwave vial and placed in the microwave oven at 300 W. After 5 minutes of heating at 100 °C without stirring, the crystalline NCP-**1** particles were isolated via centrifuge at 13,000 rpm for 15 min. The particles were washed once with dmf and three times with EtOH to afford approximately 4 mg of NCP-**1** (54.3% yield).

A typical procedure for silica coating

4 mg of NCP-**2** particles was dispersed in 10 mL of 0.2M aq. NH_3 in ethanol. 16 μL of TEOS was added to the dispersion with magnetic stirring at room temperature. After 5 h, nanoparticles were isolated by centrifuging at 13,000 rpm for 15 min, washed with dmf and ethanol, and re-dispersed in ethanol via sonication.

A typical procedure for PEGylation and targeting

The SiO_2@**2** particles were diluted with ethanol to a final concentration of 3 mg/mL. To this dispersion was added Siloxy-PEG_{2K}-anisamide and Siloxy-PEG_{2K}-OCH_3 with a molar ratio of 1 to 9 (1mg PEG/mL EtOH) and the resulting mixture was magnetically stirred under basic conditions (NH_3, 0.3 M aq.) at room temperature for 24 h. The anisamide-targeted particles were isolated via centrifugation, washed with ethanol, and redispersed in ethanol via sonication.

Supplementary Material

Refer to Web version on PubMed Central for supplementary material.

References

1. Fujimoto, J.; Farkas, D. Biomedical Optical Imaging. First ed.. New York: Oxford University Press, Inc.; 2009.
2. a) Ntziachristos V, Ripoll J, Wang LV, Weissleder R. Nat. Biotech. 2005; 23:313.b) Kobayashi H, Ogawa M, Alford R, Choyke PL, Urano Y. Chem. Rev. 2009; 110:2620. [PubMed: 20000749] c) Kim C, Favazza C, Wang LV. Chem. Rev. 2010; 110:2756. [PubMed: 20210338]
3. a) Nahrendorf M, Keliher E, Marinelli B, Waterman P, Feruglio PF, Fexon L, Pivovarov M, Swirski FK, Pittet MJ, Vinegoni C, Weissleder R. Proc. Natl. Acad. Sci. 2010; 107:7910. [PubMed: 20385821] b) Cobley CM, Chen J, Cho EC, Wang LV, Xia Y. Chem. Soc. Rev. 2011; 40:44. [PubMed: 20818451] c) Nam T, Park S, Lee SY, Park K, Choi K, Song IC, Han MH, Leary JJ, Yuk SA, Kwon IC, Kim K, Jeong SY. Bioconjug. Chem. 2010; 21:578. [PubMed: 20201550]
4. a) Kikuchi K. Chem. Soc. Rev. 2010; 39:2048. [PubMed: 20372693] b) Cheng MMC, Cuda G, Bunimovich YL, Gaspari M, Heath JR, Hill HD, Mirkin CA, Nijdam AJ, Terracciano R, Thundat T, Ferrari M. Curr. Opin. Chem. Biol. 2006; 10:11. [PubMed: 16418011] c) Haruyama T. Adv. Drug Del. Rev. 2003; 55:393.
5. a) Alivisatos P. Nat. Biotechnol. 2004; 22:47. [PubMed: 14704706] b) Gao X, Yang L, Petros JA, Marshall FF, Simons JW, Nie S. Curr. Opin. Biotechnol. 2005; 16:63. [PubMed: 15722017] c) Somers RC, Bawendi MG, Nocera DG. Chem. Soc. Rev. 2007; 36:579. [PubMed: 17387407]

6. Luminescent molecules were recently incorporated into Zr phophate nanoparticles. See: Roming M, Lünsdorf H, Dittmar KEJ, Feldmann C. Angew. Chem. Int. Ed. 2010; 49:632.
7. Phosphorescent dyes has been incorporated into silica matrices via electrostatoic interactions, albeit at much lower loadings. See: He X, Nie H, Wang K, Tan W, Wu X, Zhang P. Anal. Chem. 2008; 80:9597. [PubMed: 19007246] Lian W, Litherland SA, Badrane H, Tan W, Wu D, Baker HV, Gulig PA, Lim DV, Jin S. Anal. Biochem. 2004; 334:135. [PubMed: 15464962] Zhao X, Bagwe RP, Tan W. Adv. Mater. 2004; 16:173. Rieter WJ, Kim JS, Taylor KML, An H, Lin W, Tarrant T, Lin W. Angew. Chem. Int. Ed. 2007; 46:3680.
8. Robson R. Dalton Trans. 2008:5113. [PubMed: 18813362]
9. a) Murray LJ, Dinca M, Long JR. Chem. Soc. Rev. 2009; 38:1294. [PubMed: 19384439] b) Ma L, Mihalcik DJ, Lin W. J. Am. Chem. Soc. 2009; 131:4610. [PubMed: 19290636] c) Furukawa H, Ko N, Go YB, Aratani N, Choi SB, Choi E, Yazaydin AO, Snurr RQ, O'Keeffe M, Kim J, Yaghi OM. Science. 2010; 329:424. [PubMed: 20595583] d) Uemura K, Kitagawa S, Fukui K, Saito K. J. Am. Chem. Soc. 2004; 126:3817. [PubMed: 15038736]
10. Evans OR, Lin W. Acc. Chem. Res. 2002; 35:511. [PubMed: 12118990]
11. a) Chen B, Wang L, Xiao Y, Fronczek FR, Xue M, Cui Y, Qian G. Angew. Chem. Int. Ed. 2009; 48:500.b) Lan A, Li K, Wu H, Olson DH, Emge TJ, Ki W, Hong M, Li J. Angew. Chem. Int. Ed. 2009; 48:2334.c) Xie Z, Ma L, deKrafft KE, Jin A, Lin W. J. Am. Chem. Soc. 2009; 132:922. [PubMed: 20041656]
12. a) Ma L, Abney C, Lin W. Chem. Soc. Rev. 2009; 38:1248. [PubMed: 19384436] b) Wu C-D, Hu A, Zhang L, Lin W. J. Am. Chem. Soc. 2005; 127:8940. [PubMed: 15969557] c) Lee J, Farha OK, Roberts J, Scheidt KA, Nguyen ST, Hupp JT. Chem. Soc. Rev. 2009; 38:1450. [PubMed: 19384447] d) Song F, Wang C, Falkowski JM, Ma L, Lin W. J. Am. Chem. Soc. 2010; 132:15390. [PubMed: 20936862] e) Ma L, Falkowski JM, Abney C, Lin W. Nat. Chem. 2010; 2:838. [PubMed: 20861899]
13. a) Lin W, Rieter WJ, Taylor KML. Angew. Chem. Int. Ed. 2009; 48:650.b) Della Rocca J, Lin W. Eur. J. Inorg. Chem. 2010:3725.c) Huxford RC, Della Rocca J, Lin W. Curr. Opinion Chem. Biol. 2010; 14:262.d) Spokoyny AM, Kim D, Sumrein A, Mirkin CA. Chem. Soc. Rev. 2009; 38:1218. [PubMed: 19384433]
14. Rieter WJ, Taylor KML, Lin W. J. Am. Chem. Soc. 2007; 129:9852. [PubMed: 17645339]
15. a) Horcajada P, Chalati T, Serre C, Gillet B, Sebrie C, Baati T, Eubank JF, Heurtaux D, Clayette P, Kreuz C, Chang J-S, Hwang YK, Marsaud V, Bories P-N, Cynober L, Gil S, Ferey G, Couvreur P, Gref R. Nat Mater. 2010; 9:172. [PubMed: 20010827] b) Rieter WJ, Taylor KML, An H, Lin W, Lin W. J. Am. Chem. Soc. 2006; 128:9024. [PubMed: 16834362] c) Taylor KML, Jin A, Lin W. Angew. Chem. Int. Ed. 2008; 47:7722.
16. deKrafft KE, Xie Z, Cao G, Tran S, Ma L, Zhou OZ, Lin W. Angew. Chem. Int. Ed. 2009; 48:9901.
17. Rieter WJ, Pott KM, Taylor KML, Lin W. J. Am. Chem. Soc. 2008; 130:11584. [PubMed: 18686947]
18. Single-crystal X-ray diffractometer system equipped with a Cu-target X-ray tube (l=1.54178 Å). Crystal data for LRuZn MOF: Triclinic, space group:P-1, a = 9.4196(2) Å, b = 14.0381(4) Å, c = 18.0896(4) Å, α = 83.244(2)°, β= 75.876(2)°, γ= 76.670(2)°, V=2252.46(9) Å3, ρcalc= 1.418 g/cm3. CCDC 804313 contain the supplementary crystallographic data for this paper. These data can be obtained free of charge from The Cambridge Crystallographic Data Centre via www.ccdc.cam.ac.uk/data_request/cif.
19. Kent CA, Mehl BP, Ma L, Papanikolas JM, Meyer TJ, Lin W. J. Am. Chem. Soc. 2010; 132:12767. [PubMed: 20735124]
20. a) Fu Q, Lu C, Liu J. Nano Lett. 2002; 2:329.b) Lu Y, Yin Y, Mayers BT, Xia Y. Nano Lett. 2002; 2:183.
21. Cavka JH, Jakobsen S, Olsbye U, Guillou N, Lamberti C, Bordiga S, Lillerud KP. J. Am. Chem. Soc. 2008; 130:13850. [PubMed: 18817383]
22. Vilner BJ, John CS, Bowen WD. Cancer Res. 1995; 55:408. [PubMed: 7812973]
23. a) Li S, Chen YC, Hackett MJ, Huang L. Mol. Ther. 2008; 16:163. [PubMed: 17923843] b) John CS, Vilner BJ, Geyer BC, Moody T, Bowen WD. Cancer Res. 1999; 59:4578. [PubMed:

10493511] c) Banerjee R, Tyagi P, Li S, Huang L. Int.J. Cancer. 2004; 112:693. [PubMed: 15382053]

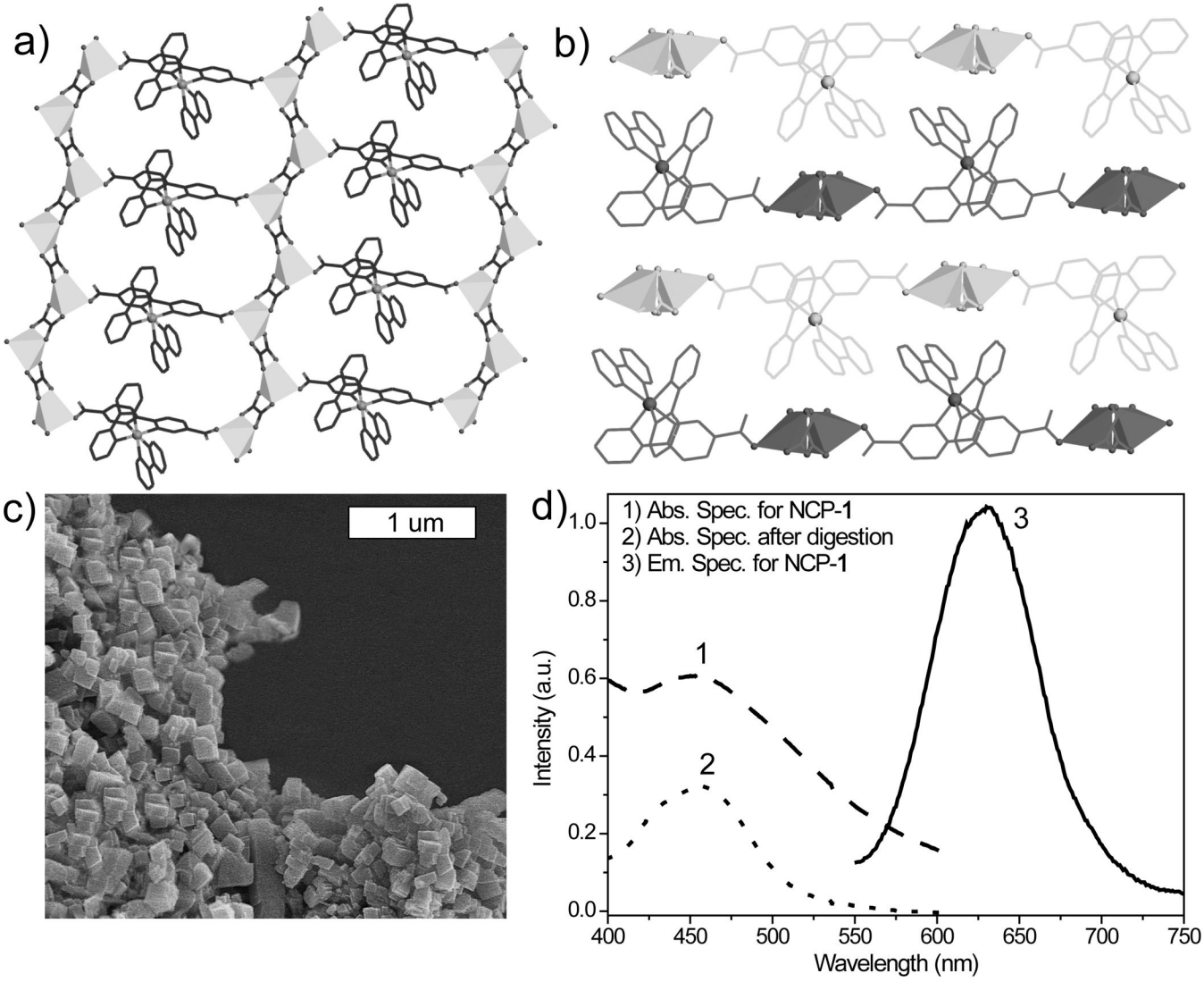

Figure 1.

a) A top view of the 2D layer of **1** down the *b* axis; b) A side view along the *a* axis showing the packing of the 2D layers in **1**; c) SEM image of NCP-**1**; d) Absorption [1] and emission [2] spectra of NCP-**1** in ethanol. The absorption spectrum of dissolved NCP-**1** [3] was also taken to eliminate the scattering effects.

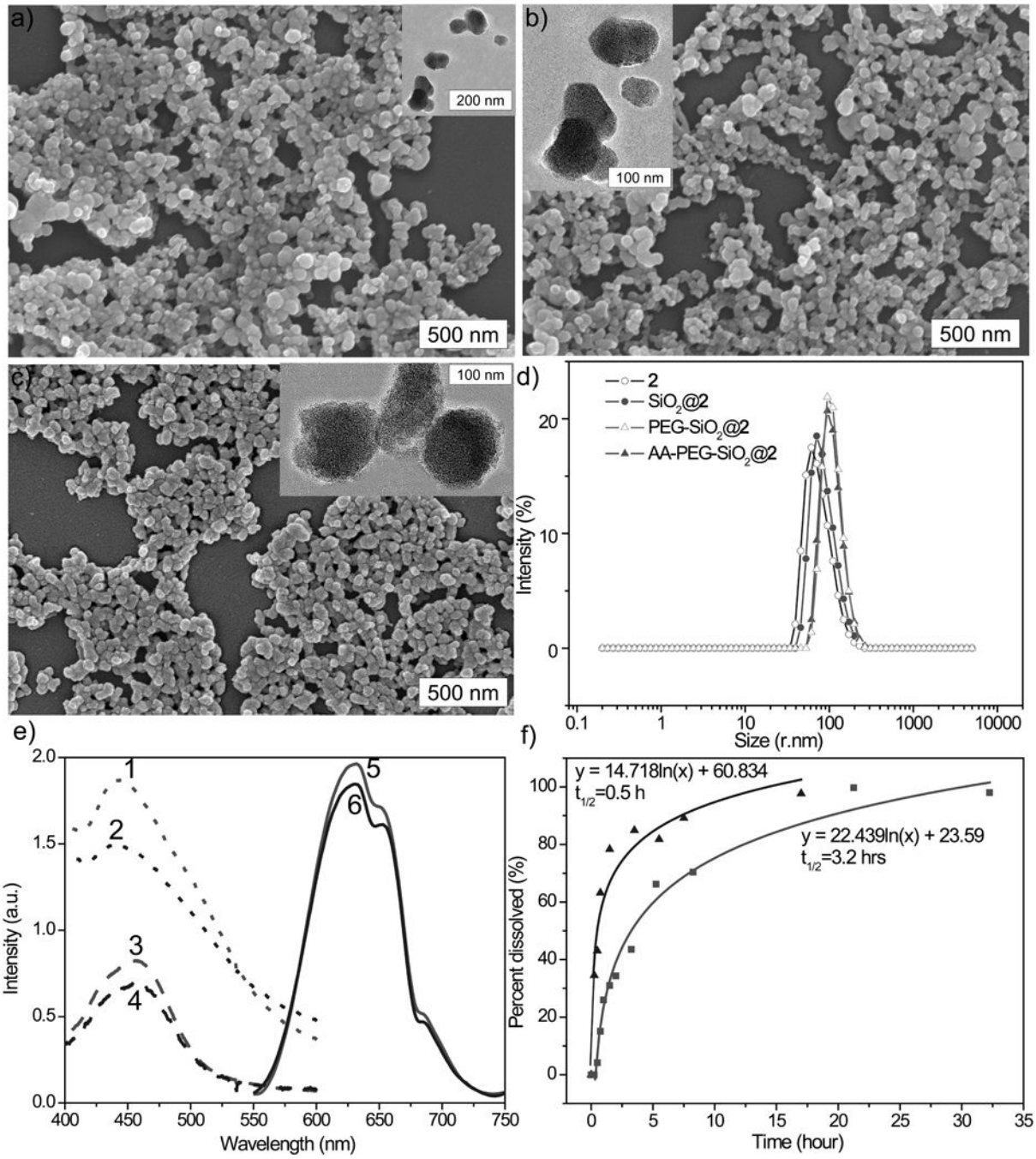

Figure 2.

SEM and TEM (inset) images of NCP-**2** (a), SiO_2@**2** (b), and AA-PEG-SiO_2@**2** (c); d) Number-averaged size distribution for NCP-**2** (open circle), SiO_2@**2** (solid circle), PEG-SiO_2@**2** (open triangle), and AA-PEG-SiO_2@**2** (solid triangle) in ethanol; e) Absorption and emission spectra: abs. spec. for NCP-**2** [1], Abs. Spec. for AA-PEG-SiO_2@**2** [2], abs. spec. for NCP-**2** after digestion [3], Abs. Spec. for AA-PEG-SiO_2@**2** after digestion [4], normalized emiss. spec. for NCP-**2** [5], normalized emiss. spec. for AA-PEG-SiO_2@**2** [6]; f) Release profiles of NCP-**2** (triangle) and SiO_2@**2** (sqaure) in 8 mM PBS at 37 °C.

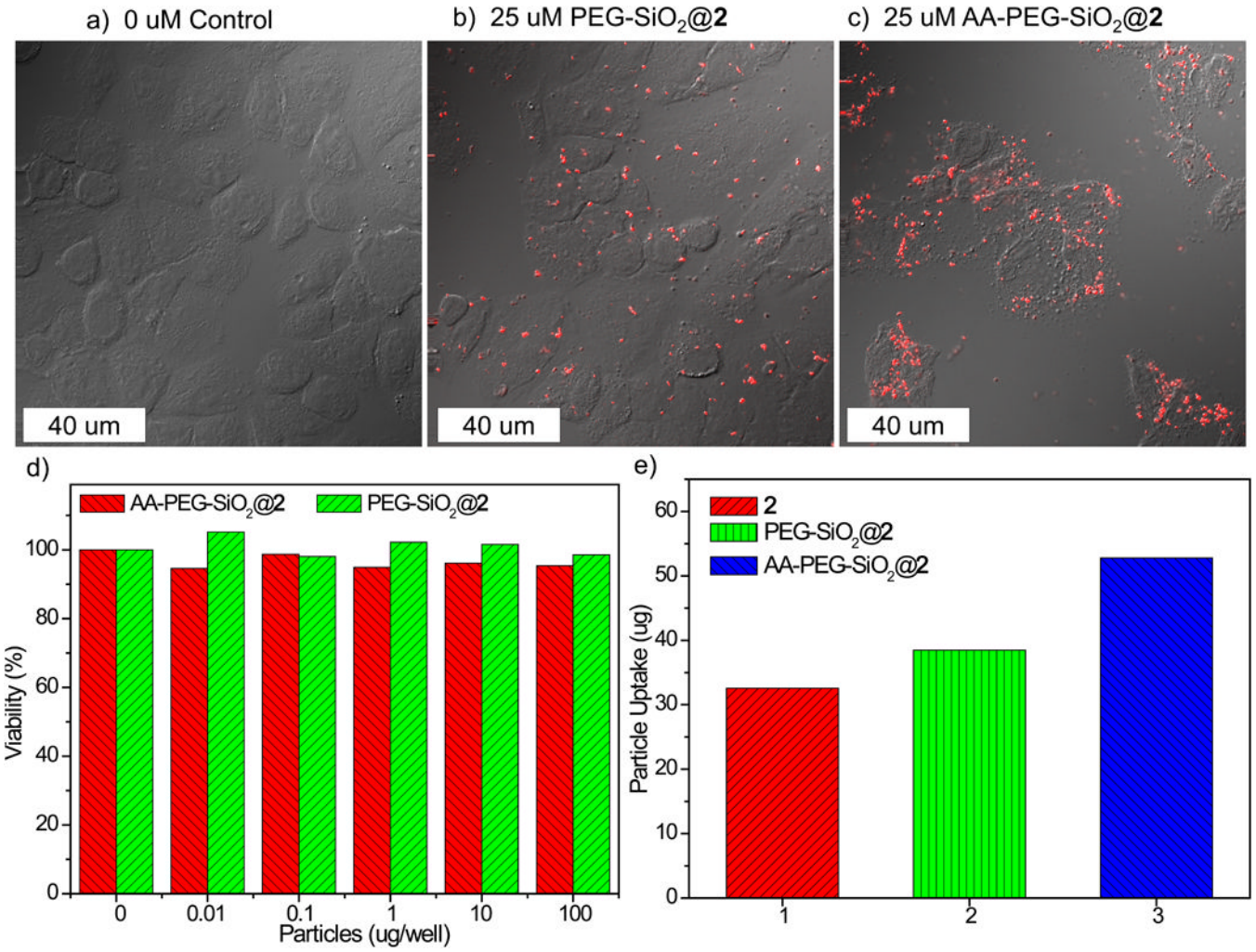

Figure 3.

Confocal microscopic images of H460 cells that have been incubated with various nanoparticles: control cells without any particles (a), cells with PEG-SiO_2@**2** (b), and cells with AA-PEG-SiO_2@**2** (c); d) *in vitro* viability assay for H460 cells incubated with various amounts of PEG-SiO_2@**2** and AA-PEG-SiO_2@**2**; e) Particle uptake studies in H460 cells.

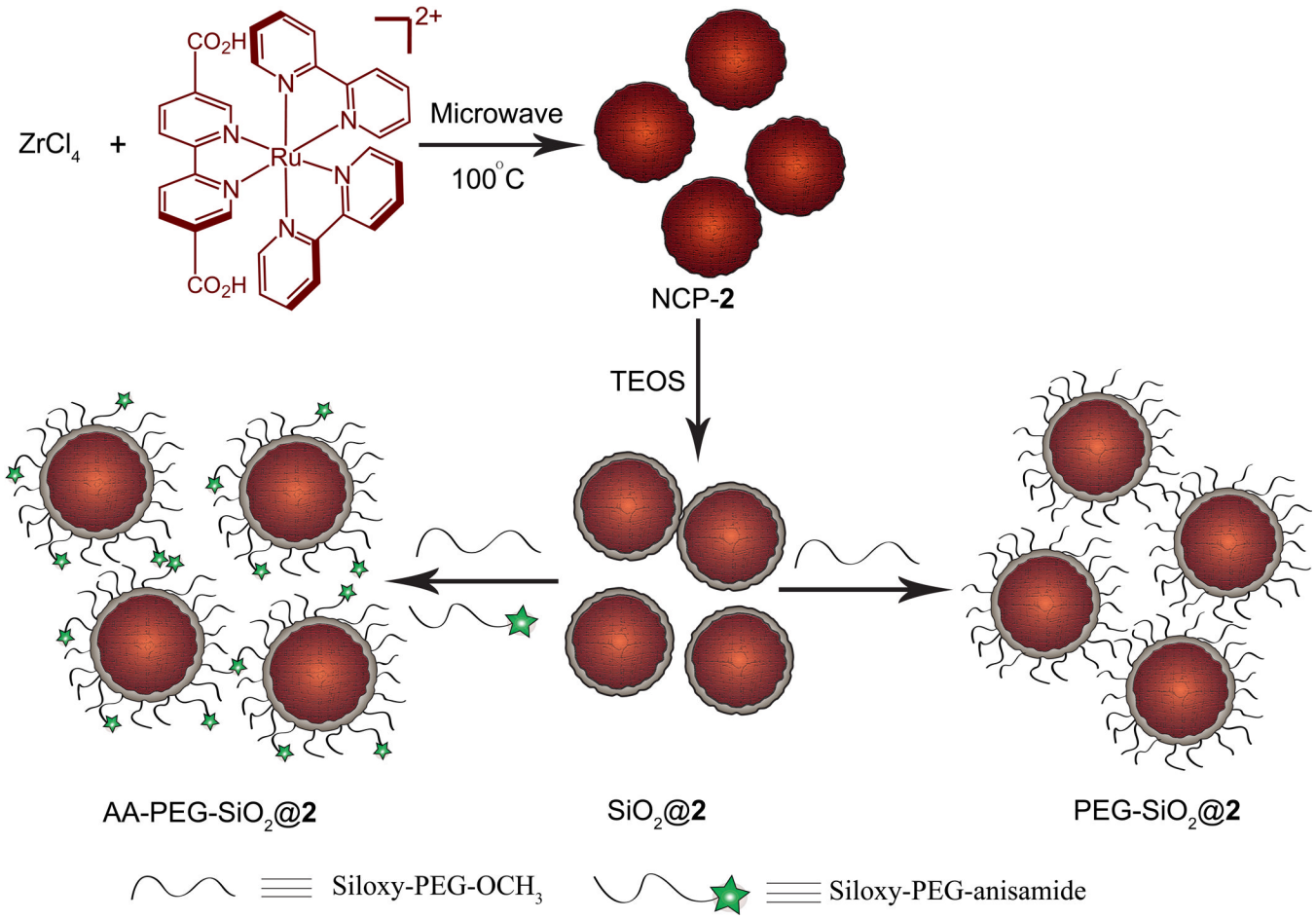

Scheme 1.
Synthesis of NCP-**2**, and coating of NCP-**2** with a thin shell of silica, and further functionalization of SiO_2@**2** with PEG and PEG-anisamide.

Table 1

Summary of characterization data for NCP-**2** and related particles.

Particle	Z-Ave diameter (nm)	PDI	Zeta Potential (mV)	Dye loading (TGA)	Dye loading (ICP-MS)
NCP-**2**	104±4	0.205	−11.9±3.2	57.4%	55.0%
SiO_2@**2**	107±4	0.135	−34.4±4.1	34.4%	28.5%
PEG-SiO_2@**2**	122±10	0.103	−9.23±1.9	32.9%	27.6%
AA-PEG-SiO_2@**2**	124±7	0.062	−8.17±2.8	32.7%	27.0%

Angew Chem Int Ed Engl. Author manuscript; available in PMC 2012 September 03.